Journal of Nuclear Materials 390–391 (2009) 440–443

Contents lists available at ScienceDirect

Journal of Nuclear Materials

journal homepage: www.elsevier.com/locate/jnucmat

The enhanced pedestal H-mode in the National Spherical Torus experiment

R. Maingi [a,*], R.E. Bell [b], B.P. LeBlanc [b], D.A. Gates [b], S.M. Kaye [b], J.E. Menard [b], S.A. Sabbagh [c], H. Yuh [d]

[a] Oak Ridge National Laboratory, Oak Ridge, c/o Princeton Plasma Physics Lab, Receiving 3, Route 1 North, Princeton, NJ 08543, USA
[b] Princeton Plasma Physics Laboratory, Princeton, NJ, USA
[c] Columbia University, New York, NY, USA
[d] Nova Photonics, Princeton, NJ, USA

ARTICLE INFO

PACS:
52.55.Fa
52.40.Hf

ABSTRACT

Typical H-mode pedestal electron and ion temperatures in NSTX range from 100–300 eV. A new operating regime termed the 'enhanced pedestal' (EP) H-mode has been observed in which the pedestal ion temperature increases to ~600 eV in about 50 ms, or one energy confinement time, resulting in a global confinement improvement. Ion temperature gradients as high as 30 keV/m are observed. The regime is correlated with a localized braking of the edge toroidal rotation near the $q = 3$ surface, in which case the pressure gradient term in the radial force balance becomes dominant over the toroidal and poloidal rotation terms. Coupled with increased rotation just inside the barrier, the radial electric field shear is also increased. An MHD trigger event (large edge localized mode) is common to the formation of the EP H-mode phase, which can occur either during the I_p ramp-up or flat-top phases of discharges. The observed characteristics of this scenario are presented.

1. Introduction

Spherical tori (ST) have demonstrated [1–5] higher β_t operation than higher aspect ratio devices, as predicted by theory [6]. Here, β_t is the magnetic field utilization: $\beta_t = 2\mu_0 W_{MHD}/B_t^2$, where W_{MHD} is the plasma stored energy, B_t is the torodial field, and μ_0 is the permeability of free space. In present-day STs, this higher β_t operation is enabled partly by operation at low B_t. For perspective, the typical $B_t = 0.45$ T in the National Spherical Torus Experiment (NSTX) [7], whereas the typical $B_t = 2.1$ T in the DIII-D device, which operates at twice the major radius and aspect ratio of NSTX. A possible consequence of the parameter regime in which STs operate is relatively low H-mode pedestal temperatures, as also predicted by some theories [8]. Indeed, typical H-mode pedestal electron and ion temperatures ($T_{e,i}^{ped}$) in the NSTX and the Mega-Amp Spherical Tokamak (MAST) range from 100–300 eV [9,10].

However, a new operating regime has been observed in NSTX in which the T_i^{ped} and T_e^{ped} spontaneously increased to ~600 eV in about 50 ms, or one energy confinement time, resulting in a global energy confinement (τ_E) improvement. Specifically the energy confinement relative to the global ITER-97 L-mode scaling [11], $\tau_E/\tau_E^{ITER97\text{-}L}$, increased up to 2.5. Ion temperature radial gradients as high as 30 keV/m were measured. Even though the new regime is presently transient, it represents a promising approach to improved edge and core performance, if extensible.

2. Characteristics of enhanced pedestal H-mode

The evolution of two discharges, a standard H-mode and an enhanced pedestal (EP) H-mode, are compared in Fig. 1. Both discharges were inductively ramped to a plasma current (I_p) of 1 MA (panel (a)), and neutral beam injected (P_{NBI}) power of 4 MW was delivered during the I_p ramp. Both discharges exhibited a drop in divertor D_α emission at ~130 ms, indicative of an L–H transition (panel (d)), and a D_α spike at ~170 ms. The stored energy (W_{MHD}) from equilibrium reconstructions [12] approached ~80 kJ in both discharges by 170 ms (panel (b)), although the time dependence was different, partly related to the details of the reconstruction and other factors. Following the D_α spike at ~170 ms, the W_{MHD} in the EP H-mode discharge ramped up at a rapid rate, specifically $dW_{MHD}/dt \sim 0.4 \times P_{NBI}$. This large dW_{MHD}/dt translated into a substantial improvement in the energy confinement time, up to 50% higher than the standard H-mode discharge before the collapse of the EP H-mode discharge at about 260 ms in panel (c).

EP H-mode phases have been observed both during I_p ramp-up (e.g. Fig. 1) and during the I_p flat-top phase in other discharges (not shown). A common signature is a spike in the D_α emission, which is caused by a large edge localized mode (ELM). The collapse of the EP H-mode discharge shown above was correlated with the onset of a locked mode when the normalized β_N ($\beta_N = aB_t\beta_t/I_p$ with $a \cong$ minor radius) exceeded ~4.5. This global β_N limit was verified in other discharges with higher P_{NBI}, which showed a more rapid dW_{MHD}/dt but the same β_N limit. This limit on β_N is lower than the normal

* Corresponding author.
E-mail address: rmaingi@pppl.gov (R. Maingi).

0022-3115/$ - see front matter © 2009 Elsevier B.V. All rights reserved.
doi:10.1016/j.jnucmat.2009.01.126

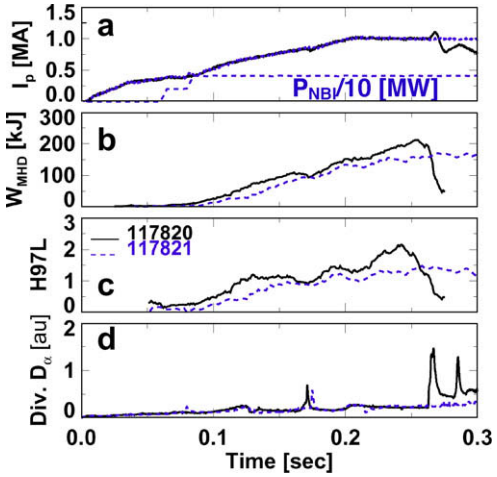

Fig. 1. Time evolution of a discharge with transition to enhanced pedestal H-mode (solid black) and a standard H-mode discharge (dashed blue): (a) I_p and the P_{NBI} waveform common to both discharges, (b) W_{MHD}, (c) confinement enhancement factor relative to the ITER-97 L-mode scaling, and (d) divertor D_α emission.

$\beta_N^{max} \sim 5.5$–6 in standard H-mode discharges, because these particular EP H-mode discharges exhibited extremely reversed shear of the current profile during the I_p ramp. Occurrences of EP H-modes during the steady I_p phase have exhibited higher β_N^{max} values, demonstrating that the regime does not have an intrinsic $\beta_N^{max} \sim 4.5$. While the effect on stored energy and confinement is moderate, the modification of the plasma kinetic radial profiles is striking and discussed in detail below.

3. Kinetic profile evolution and comparison between ordinary H-mode and EP H-mode

The electron density, electron temperature, ion temperature, and toroidal rotation profiles (n_e, T_e, T_i, v_{tor}) from Thomson scattering and Charge Exchange Recombination Spectroscopy (ChERS) measurements are compared between the standard H-mode (blue triangles) and the EP H-mode (black circles) discharge in Fig. 2 at a time just before the collapse of the EP H-mode. One dramatic difference is an apparent 3–5 cm radial inward movement of the plasma boundary during the EP H-mode phase. Just inside of the inward shifted boundary, however, sharp gradients in T_e and T_i were observed in the EP H-mode phase, leading to higher central values of T_e and T_i than in the standard H-mode discharge. The n_e profile was unchanged except for the inward boundary shift in the EP H-mode phase, and the v_{tor} profile was modified from a monotonically decreasing profile to one which had a minimum in the T_i steep gradient region. Outside of the steep gradient region, v_{tor} increased again. We note that similar v_{tor} profiles have been observed when an edge island becomes large enough to slow down the edge rotation in standard H-mode discharges; in the EP H-mode phase, the spatial location of the velocity minimum corresponded approximately to the $q = 3$ surface.

The evolution of the n_e, T_e, T_i, v_{tor} profiles during the EP H-mode phase is shown in more detail in Fig. 3. The first set of profiles at 0.165 sec are typical H-mode profiles, with $\sim T_e^{ped} \sim 150$ eV and no clear pedestal in the T_i profile. The profile evolution following the MHD event was gradual: the boundary shifted inward continuously while the T_e and T_i gradients increased with time. Note the n_e^{ped} value remained constant at between 4 and 5×10^{19} m^{-3}, with the pedestal top location moving radially inward with time. The v_{tor} profile (not shown) exhibited a minimum near 0 m/s; the loca-

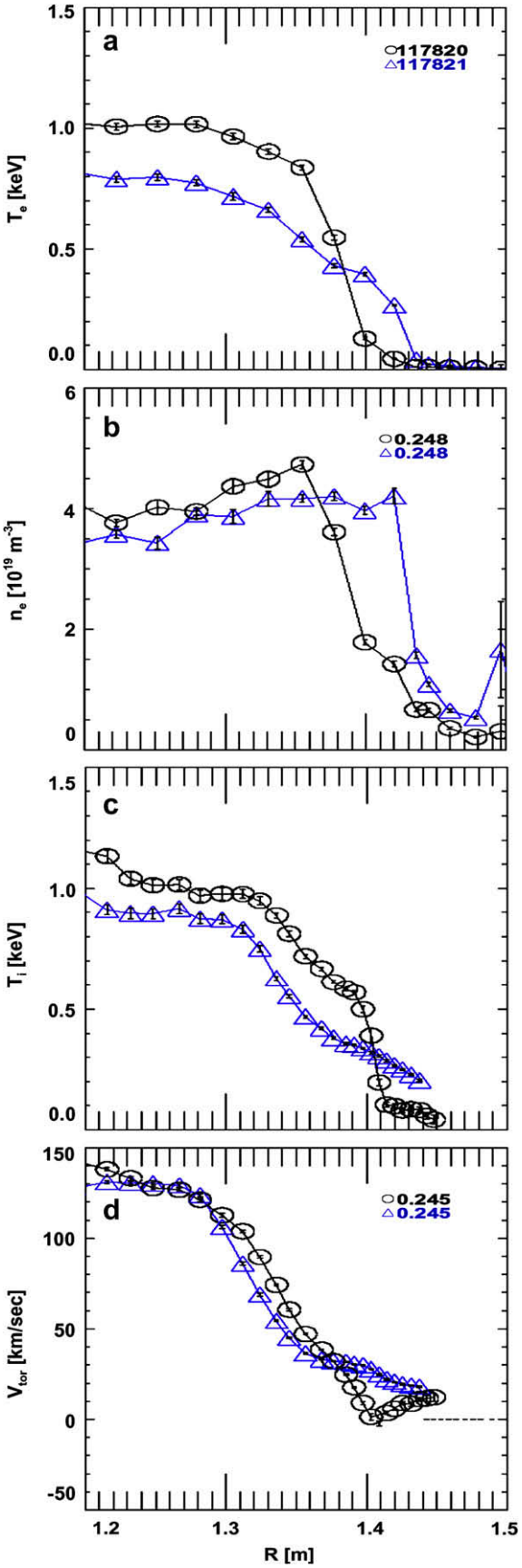

Fig. 2. Profile comparison of n_e, T_e, T_i, and v_{tor} between EP H-mode (black circles) and standard H-mode (blue triangles). (For interpretation of the references to colours in this figure, the reader is referred to the web version of this paper.)

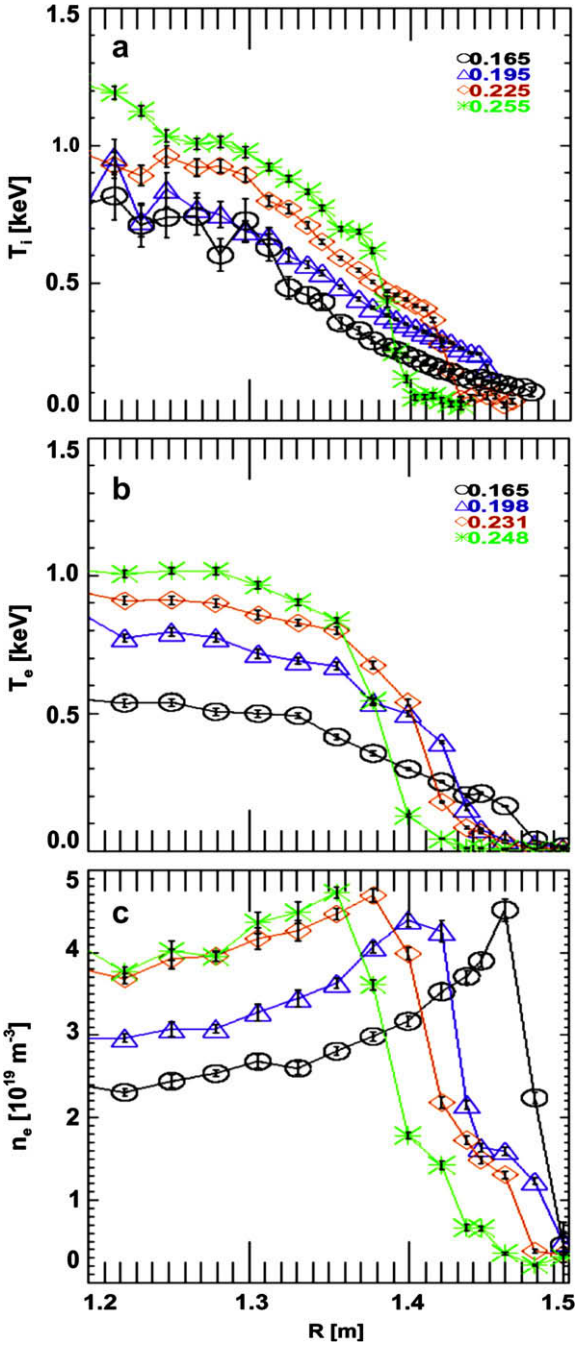

Fig. 3. Profile evolution n_e, T_e, T_i, and v_{tor} during EP H-mode, showing a continuous inward movement of the plasma boundary and rising edge and core temperatures.

tion of the minimum velocity also moved radially inward with time. During the latter part of the EP H-mode phase, the edge rotation from $R = 1.25$–1.35 m actually increased, leading to a larger rotation shear than that at earlier times.

The spatial resolution of the ChERs system allows evaluation of the T_i profile characteristics using the common modified hyperbolic tangent fitting function [13]. Fig. 4 shows that the T_e^{ped} increased from 300 eV up to 650 eV by the end of the EP H-mode phase, whereas the width decreased to between 1 and 1.8 cm. At the narrowest point at 0.235 s, the width was the equivalent of approximately two ion Larmor radii for the T_i value at the midpoint of the steep gradient region. Note that the radial T_i gradient increased to 30 keV/m.

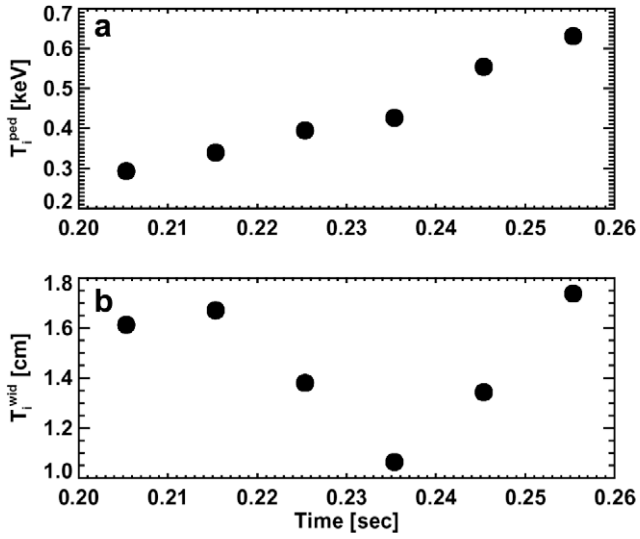

Fig. 4. Evolution of T_i^{ped} and the width of the barrier (T_i^{wid}) in the EP H-mode.

4. Role of rotation and radial electric field

The components of the radial electric field, E_r, can be evaluated from the lowest order radial force balance for a given species: $E_r = v \times B - dp/dr$. In practice E_r is evaluated for the C6+ ion: $E_r = v_{tor}B_{pol} - v_{pol}B_{tor} - dp_i/dr$, where B_{pol} is the polodial field, v_{pol} is the poloidal rotation, and dp_i/dr is the ion radial pressure gradient. When these discharges were conducted, the poloidal rotation term was not measured, and so a comparison of $E_r + v_{pol}B_{tor}$ is given in

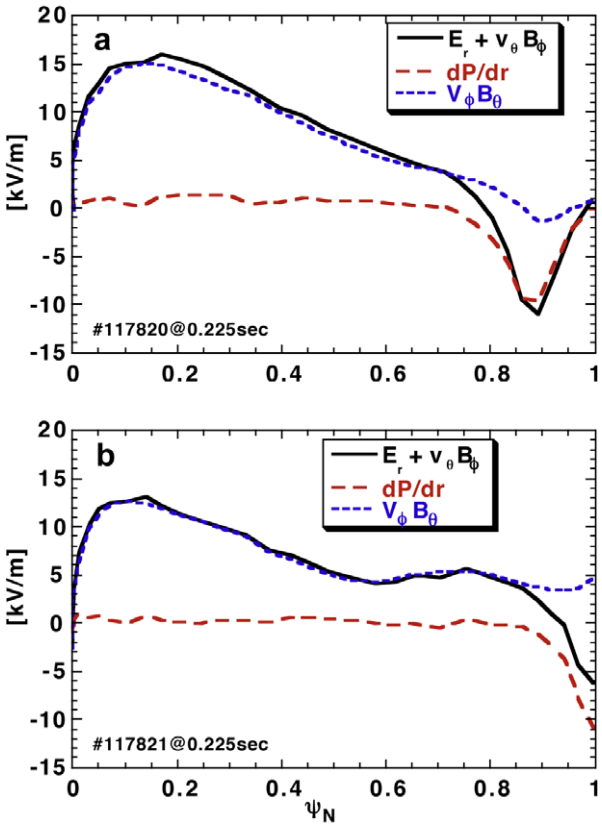

Fig. 5. Components of the E_r profile during the EP H-mode and the regular H-mode. The EP H-mode shows a broader region of E_r shear. Subsequent measurements have shown that the poloidal rotation v_θ is near 0 in the EP H-mode phase, such that the black line is nearly equal to E_r. (For interpretation of the references to colours in this figure, the reader is referred to the web version of this paper.)

Fig. 5 for the standard H-mode and EP H-mode discharges. Here, the impact of the local minimum in v_{tor} becomes evident: in the steep gradient region, the pressure gradient term substantially exceeds the v_{tor} term (which approaches 0), leading to a broad region of large E_r and E'_r from ψ_N of 0.8–1.0. Subsequent to this set of discharges, the poloidal rotation velocity was measured to be very close to 0 in EP H-mode phases, such that E_r became largely determined by the pressure gradient term.

5. Summary and conclusions

The EP H-mode is a spontaneously occurring phase of discharges with increased pedestal temperatures and pressures, and improved global confinement. A large ELM is observed before all EP H-mode phases and is hypothesized to trigger the transport change. The edge of the plasma moves radially inward continuously during the EP H-mode phase, and a drag is observed on the edge toroidal rotation velocity, which approaches zero near the $q = 3$ surface. The first order radial force balance indicates that the pressure gradient term dominates the other terms, leading to a large region of E_r shear, which may be responsible for the reduced transport and improved confinement. We thus conjecture the following physics picture for the EP H-mode triggering: (1) the ELM rapidly reduces edge v_{tor}, leading to a large E'_r and the transition to improved confinement; and (2) the local island breaking near the $q = 3$ surface maintains a steep v'_{tor} and E'_r, which allows confinement to increase on a transport time scale. Both of these mechanisms appear necessary, which explains why EP H-mode was not observed for the control shot in Fig. 1 (no island breaking).

At present the EP H-mode has only been observed as a transient phase in H-mode discharges. If the key physics is indeed a local toroidal breaking leading to an enhanced edge transport barrier, then the prospect of triggering such barriers on demand with non-axisymmetric magnetic perturbations is conceivable. Such perturbations have been shown to brake the toroidal rotation at rates given by neoclassical theory [14]. Reproducing the localized island braking would likely require a high toroidal mode number perturbation. Future work will also focus on the requirements for externally generated perturbations to reproduce the braking effects observed here with island braking.

Acknowledgements

This research was supported by the US Department of Energy under Contracts DE-AC05-00OR22725, and DE-AC02-76CH03073, and Grants DE-FG02-99ER54524 and DE-FG02-04ER54767. We gratefully acknowledge the contribution of the NSTX technical staff and operations staff.

References

[1] M. Gryaznevich et al., Phys. Rev. Lett. 80 (1998) 3972.
[2] D.A. Gates et al., Phys. Plasma 5 (1998) 1775.
[3] S.A. Sabbagh et al., Phys. Plasma 9 (2002) 2085.
[4] D.A. Gates et al., Phys. Plasma 10 (2003) 1659.
[5] J.E. Menard et al., Nucl. Fus. 43 (2003) 330.
[6] J.E. Menard et al., Nucl. Fus. 37 (1997) 595.
[7] M. Ono, S.M. Kaye, Y.-K.M. Peng, et al., Nucl. Fus. 40 (2000) 557.
[8] P.N. Guzdar et al., Phys. Plasma 12 (2005) 032502.
[9] R. Maingi, C.E. Bush, E.D. Fredrickson, et al., Nucl. Fus. 45 (2005) 1066.
[10] A. Kirk et al., Plasma Phys. Control. Fus. 46 (2004) A187.
[11] S.M. Kaye, M. Greenwald, U. Stroth, et al., Nucl. Fus. 37 (1997) 1303.
[12] S.A. Sabbagh, S.M. Kaye, J. Menard, et al., Nucl. Fus. 41 (2001) 1601.
[13] R.J. Groebner et al., Plasma Phys. Control. Fus. 40 (1998) 673.
[14] W. Zhu, S.A. Sabbagh, R.E. Bell, et al., Phys. Rev. Lett. 96 (2006) #225002.